ARTICLE

doi:10.1038/nature09591

Direct conversion of human fibroblasts to multilineage blood progenitors

Eva Szabo[1], Shravanti Rampalli[1], Ruth M. Risueño[1], Angelique Schnerch[1,2], Ryan Mitchell[1,2], Aline Fiebig-Comyn[1], Marilyne Levadoux-Martin[1] & Mickie Bhatia[1,2]

As is the case for embryo-derived stem cells, application of reprogrammed human induced pluripotent stem cells is limited by our understanding of lineage specification. Here we demonstrate the ability to generate progenitors and mature cells of the haematopoietic fate directly from human dermal fibroblasts without establishing pluripotency. Ectopic expression of OCT4 (also called POU5F1)-activated haematopoietic transcription factors, together with specific cytokine treatment, allowed generation of cells expressing the pan-leukocyte marker CD45. These unique fibroblast-derived cells gave rise to granulocytic, monocytic, megakaryocytic and erythroid lineages, and demonstrated *in vivo* engraftment capacity. We note that adult haematopoietic programs are activated, consistent with bypassing the pluripotent state to generate blood fate: this is distinct from haematopoiesis involving pluripotent stem cells, where embryonic programs are activated. These findings demonstrate restoration of multipotency from human fibroblasts, and suggest an alternative approach to cellular reprogramming for autologous cell-replacement therapies that avoids complications associated with the use of human pluripotent stem cells.

Mechanisms that govern induced pluripotent stem cell (iPSC) reprogramming from human fibroblasts remain poorly understood[1]. The process is further complicated by cellular intermediates that fail to establish a stable pluripotent state, potentially due to the inability to establish the ideal expression context of reprogramming factors to complete pluripotency induction[2–5]. These intermediates co-express genes associated with several differentiated lineages (neurons, epidermis and mesoderm)[4,5], raising the possibility that under unique conditions, fibroblasts could be induced to differentiate towards specified lineages. This maybe akin to recent demonstrations where fibroblasts were converted into single cell types, such as neurons, cardiomyocytes and macrophage-like cells[6–8]. While these studies have examined fibroblast conversion in the murine model, a similar process remains to be extrapolated towards human applications.

Our preliminary observations indicated that human dermal fibroblasts (Fibs) predominantly expressing OCT4 during the pluripotent reprogramming process express lineage differentiation markers that include the human pan-haematopoietic marker CD45. While both OCT2 (also called POU2F2) and OCT1 (also called POU2F1) bind similar DNA target motifs to OCT4 (ref. 9), and play a role in lymphoid development[10–12], OCT4 is yet to be implicated in haematopoiesis. Here, by ectopic expression of the POU protein OCT4, we demonstrate and characterize direct haematopoietic fate conversion to multipotent blood progenitors from fibroblasts in the human.

Emergence of CD45$^+$ cells from Fibs

Reprogramming towards pluripotency requires a cascade of events that encompasses generation of various intermediate cells among a rare subset of stable iPSCs capable of teratoma formation[13,14] (Supplementary Fig. 1a–c). A portion of these intermediates form colonies that possess round cellular morphology resembling haematopoietic cells (Supplementary Fig. 2a), and express the human pan-haematopoietic marker CD45 (CD45$^+$), but lack pluripotency marker Tra-1-60 (ref. 2) that is indicative of iPSCs (Supplementary Fig. 2b, c). These Fib-derived CD45$^+$ cells preferentially express OCT4 while demonstrating low levels of SOX2 and NANOG (Supplementary Fig. 2d, e). This suggested that Fib-derived intermediates could acquire a distinct lineage phenotype.

On the basis of these results, we compared the role of OCT4 during colony emergence from two sources of Fibs (adult dermal and neonatal foreskin) with that of NANOG or SOX2 alone (Fig. 1a). Transduced versus untransduced Fibs were examined between 14 and 21 days post-transduction (D14–D21; Supplementary Fig. 3). Unlike untransduced Fibs, or Fibs transduced with SOX2 (Fibs^{SOX2}) or NANOG (Fibs^{NANOG}), Fibs expressing OCT4 (Fib^{OCT4}) gave rise to colonies (Fig. 1a, Supplementary Fig. 3b) and exhibited OCT4 expression at levels similar to those detected in established iPSCs (Fig. 1b). Fibs^{OCT4} exclusively gave rise to haematopoietic-like CD45$^+$ cells (Fig. 1c). Furthermore, CD45$^+$ cells (CD45$^+$Fibs^{OCT4}) showed an increase in OCT4 expression (Supplementary Fig. 3c) with a concomitant decrease in the fibroblast specific gene expression[15] (Fig. 1d). Approximately 1,000 genes were downregulated and an equal number upregulated at D4, resulting in a shift towards the FibCD45$^+$ phenotype (Supplementary Table 1). To characterize and enhance emergence of CD45$^+$ Fibs, we used Flt3 (FMS-like tyrosine kinase 3) ligand and SCF (stem cell factor), representing inductive growth factors essential for early haematopoiesis[16,17]. Treatment with FLT3LG and SCF increased the frequency of CD45$^+$ colony emergence from Fibs^{OCT4} by 4 to 6-fold, compared with untreated Fibs^{OCT4} (Fig. 1e, f), while no effect was detected from control Fibs (Fig. 1e, f, Supplementary Fig. 4). These data indicate that OCT4 is sufficient to initiate emergence of CD45$^+$ cells from multiple sources of Fibs that are responsive to stimulation by early haematopoietic growth factors.

Conversion to CD45$^+$ does not require iPSCs

Ectopic expression of OCT4 alone has been shown to result in pluripotent reprogramming of neural progenitors[18]. Accordingly, we examined the expression of a panel of genes known to be essential

[1]Stem Cell and Cancer Research Institute, McMaster University, Hamilton, Ontario, Canada L8N 3Z5. [2]Department of Biochemistry and Biomedical Sciences, McMaster University, Hamilton, Ontario, Canada L8N 3Z5.

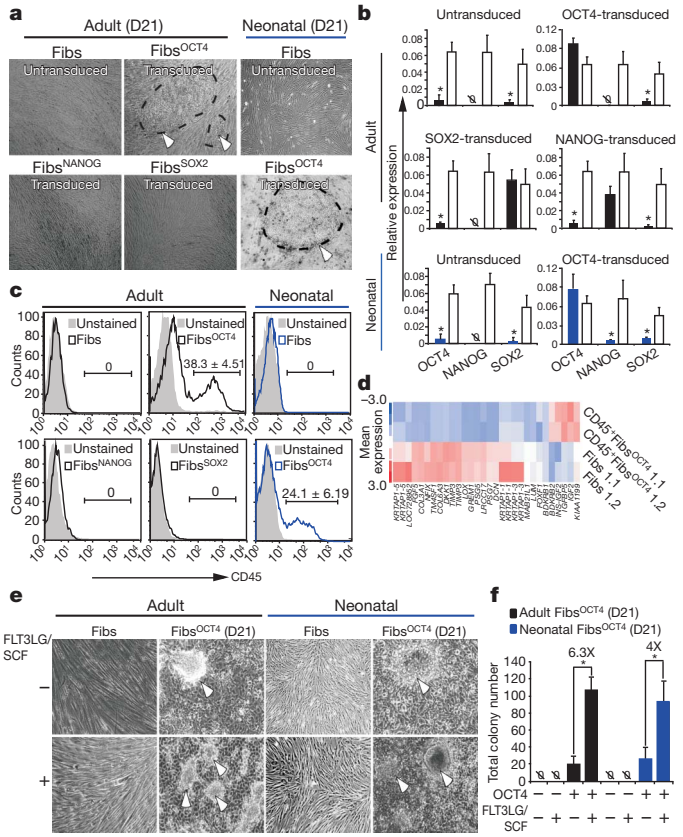

Figure 1 | OCT4 transduced human fibroblasts give rise to CD45^{+ve} colonies. **a**, Bright field images of adult and neonatal untransduced (Fibs) and OCT4- (Fibs^{OCT4}), SOX2- (Fibs^{SOX2}) or NANOG- (Fibs^{NANOG}) transduced Fibs at D21 (colonies, dashed lines and arrows) ($n = 6$). **b**, Relative gene expression at D21 of SOX2, NANOG and OCT4 in untransduced and transduced Fibs (shaded bars) in comparison with iPSCs (open bars; $n = 3$, $^*P < 0.001$). **c**, FACS analysis of CD45 (pan-haematopoietic marker) levels at D21 in transduced and untransduced adult and neonatal Fibs ($n = 6$). **d**, Global gene analysis of fibroblast marker expression of Fibs at D0 versus D21. **e**, **f**, Bright field images (**e**) and enumeration of colonies (**f**) in adult and neonatal Fibs and Fibs^{OCT4} with and without Flt3 and SCF (six biological replicates; colonies, white arrows; error bars, s.e.m.; $^*P < 0.001$).

for induction and maintenance of pluripotency[14] during emergence of CD45$^+$ Fibs. Apart from upregulation of OCT4 (Supplementary Fig. 5a), OCT4 transduction did not alter the pluripotency gene expression profile (Fig. 2a, b). Furthermore, related POU family members OCT2 and OCT1 remained unaffected (Supplementary Fig. 5b). On ectopic expression of OCT4 alone, pluripotency markers SSEA3 or Tra-1-60 were not detectable from Fibs^{OCT4}, whereas both gradually increased during establishment of iPSCs (Fig. 2c, d, Supplementary Fig. 5c–e). Unlike the fully reprogrammed hiPSCs ($n = 8$), injection of an equal number of OCT4-transduced or untransduced Fibs ($n = 6$) into immunodeficient mice failed to give rise to teratomas containing all three germ layers (Fig. 2e). Moreover, neither Fibs nor CD45$^+$Fibs^{OCT4} were immortalized, but could be maintained for approximately seven passages (Supplementary Fig. 6a), without elevation of MYC oncogene[19] (Supplementary Fig. 6b). Accordingly, our results indicate that the Fib^{OCT4} cells manifest a haematopoietic cell fate without the detectable phenotype or functional properties of transformed or pluripotent cells.

Haematopoietic progenitor of CD45 $^+$Fibs^{OCT4}

Global gene expression analysis indicated that the CD45$^+$Fibs^{OCT4} cluster with mononuclear cells derived from mobilized peripheral blood (MPB)- and umbilical cord blood (UCB)-derived haematopoietic progenitors (CD34$^+$ cells) (Supplementary Fig. 7a, b), suggesting that

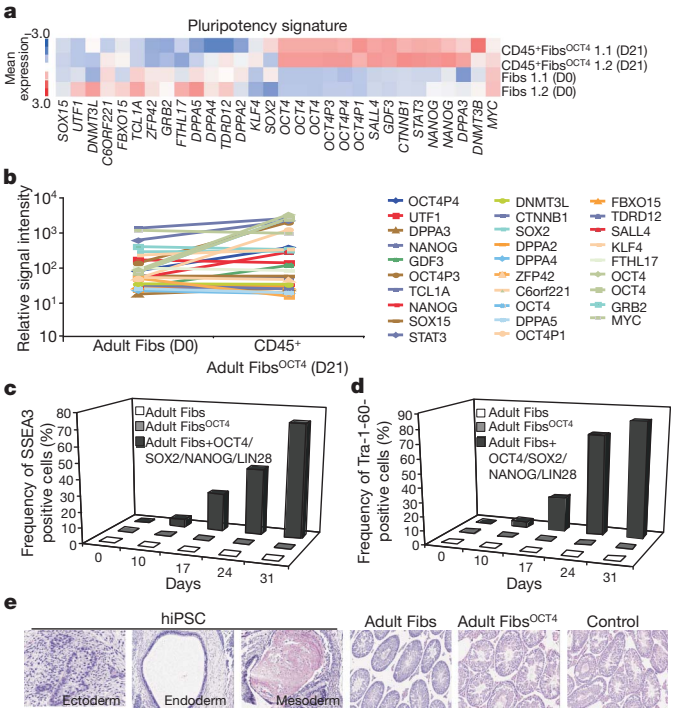

Figure 2 | OCT4 transduced dermal fibroblasts bypass the pluripotent state. **a**, Pluripotency gene signature at D0 versus D21. **b**, Pluripotency marker levels over D0 to D21. **c**, **d**, Quantitative analysis of SSEA3 (**c**) and Tra-1-60 (**d**) in Fibs, Fibs^{OCT4} with and without SCF and FLT3LG, and Fibs transduced with OCT4, SOX2, NANOG, LIN28, over the human iPSC derivation timeline ($n = 3$). **e**, Teratomas derived from human iPSCs and testicular sections from mice injected with Fibs and Fibs^{OCT4} (Control, saline injected).

CD45$^+$Fibs^{OCT4} may possess functional haematopoietic potential of multiple blood cell types. To functionally characterize haematopoietic capacity, both adult and neonatal CD45$^+$Fibs^{OCT4} were physically isolated and cultured with a cytokine cocktail known to support human haematopoietic progenitor development (Fig. 3a) and expansion (Supplementary Fig. 7c, d). The resulting progeny retained CD45 expression and acquired myeloid-specific markers CD33 and CD13 (Fig. 3b and Supplementary Fig. 8). A subfraction of CD45$^+$Fibs^{OCT4} progeny included monocytes expressing CD14 (Fig. 3c, d, Supplementary Fig. 9a) that could be further stimulated by M-CSF and IL-4 to mature into macrophages capable of phagocytosis[20]. CD45$^+$Fibs^{OCT4}-derived monocytes engulfed FITC-labelled latex beads (Fig. 3e, f, Supplementary Fig. 9b), unlike untransduced cytokine treated Fibs (Fig. 3e). Haematopoietic cytokine-treated CD45$^+$Fibs^{OCT4} derived from multiple sources of Fibs (adult and neonatal) also gave rise to granulocytic cell types distinct from monocytes (Supplementary Fig. 10a), as indicated by expression of CD15 (Fig. 3g, Supplementary Fig. 10b) and by characteristic cellular and polynuclear morphologies associated with neutrophils, eosinophils and basophils (Fig. 3h, Supplementary Fig. 10c). Without cytokines, CD45^{+ve}Fibs^{OCT4} cells retained CD45 expression, however, myeloid-specific markers were reduced and monocytic and granulocytic lineages were absent (Supplementary Fig. 11a, b). These results indicate that cytokine stimulation is necessary for haematopoietic expansion and maturation from CD45$^+$Fibs^{OCT4}.

Approximately one-quarter of cytokine-stimulated CD45$^+$Fibs^{OCT4} co-expressed CD34 (Fig. 3i, Supplementary Fig. 12). In a fashion similar to somatic UCB-derived progenitors, CD45$^+$Fibs^{OCT4} gave rise to colony forming units (CFUs), indicative of the clonal proliferative developmental potential of unipotent and bipotent progenitors of the granulocytic and macrophage lineages (Fig. 3j–l). On the basis of this *in vitro* myeloid capacity, CD45$^+$Fibs^{OCT4} progeny were transplanted into immunodeficient NOD/SCID IL2Rγc-null (NSG) mice to characterize

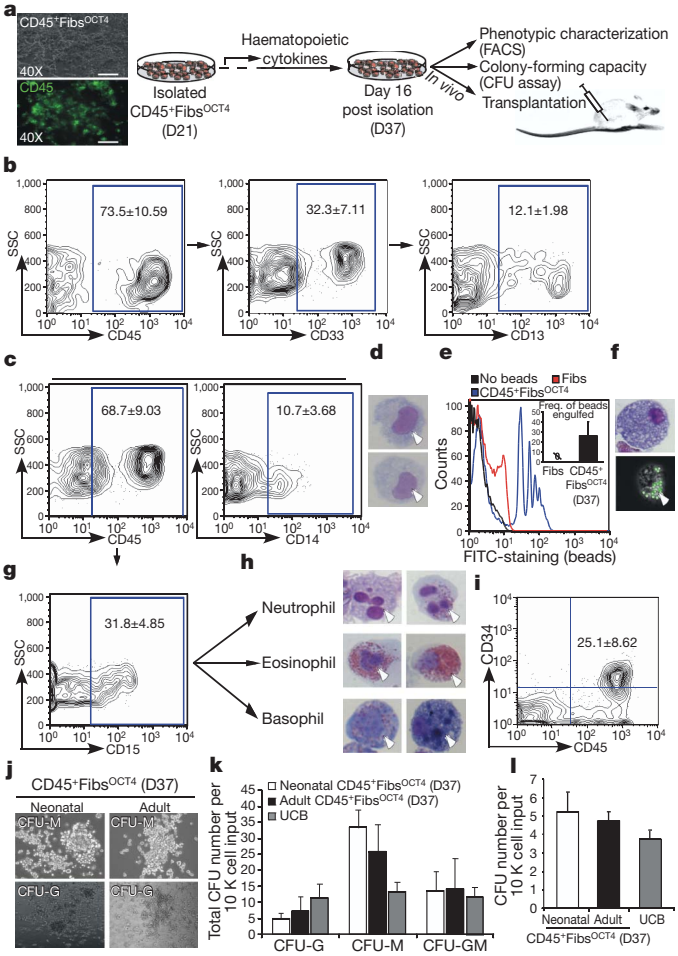

Figure 3 | *In vitro* generation of myeloid lineages from CD45$^+$ Fibs a, Schema presenting myeloid lineage derivation from CD45$^+$FibsOCT4. **b**, FACS analysis of myeloid cells derived from CD45$^+$FibsOCT4 ($n = 6$). **c**, FACS analysis of monocytes and **d**, Giemsa-Wright images of monocytes (white arrow) derived from CD45$^+$FibsOCT4 ($n = 6$). **e**, FACS analysis of macrophages, using FITC-labelled latex-bead uptake; inset shows quantitative analysis ($n = 3$). **f**, Giemsa-Wright stained image and immunofluorescence image of FITC-beads engulfed by macrophages (white arrow). **g**, FACS analysis of granulocytes derived from CD45$^+$FibsOCT4 ($n = 6$). **h**, Giemsa-Wright stained granulocytes containing neutrophils, eosinophils and basophils (white arrows) ($n = 6$). **i**, CD45$^+$FibsOCT4 derived haematopoietic progenitors ($n = 9$). **j**, Images of granulocytic (CFU-G), monocytic (CFU-M) CFUs (20×). **k**, Quantification of granulocytic, monocytic and mixed granulocytic and monocytic (CFU-GM) CFU formation from CD45$^+$CD34$^+$ cells derived from adult and neonatal Fibs and UCB ($n = 3$). **l**, CFU frequency of adult and neonatal CD45$^+$FibsOCT4 and UCB derived haematopoietic progenitors ($n = 3$; $^*P < 0.001$). Error bars, s.e.m.

their *in vivo* potential (Fig. 4a). CD45$^+$FibsOCT4-derived cells engrafted all transplanted NSG recipients up to levels of 20%, as indicated by HLA-A/B/C$^+$ cells (Fig. 4b), while Fibs and saline showed no engraftment (Fig. 4c). Engraftment levels of CD45$^+$FibsOCT4 were comparable to UCB-derived progenitors and MPB-derived progenitors (Fig. 4d). Primary reconstituted NSG recipients exhibited a predominantly myeloid phenotype (~41% CD45$^+$CD14$^+$) (Fig. 4c), compared with UCB and MPB cells (Fig. 4e). A proportion of the engrafted cells retained CFU initiation potential similar to cells from human UCB (Fig. 4f, Supplementary Fig. 13a–d). The ability to generate haematopoietic progenitors and the presence of engraftment, albeit at low levels, in the contralateral bones of the primary NSG recipients at 10 weeks post transplant (Supplementary Fig. 14a) supports the *in vivo* functional capacity of CD45$^+$FibsOCT4-derived cells. Engrafted CD45$^+$ cells were only capable

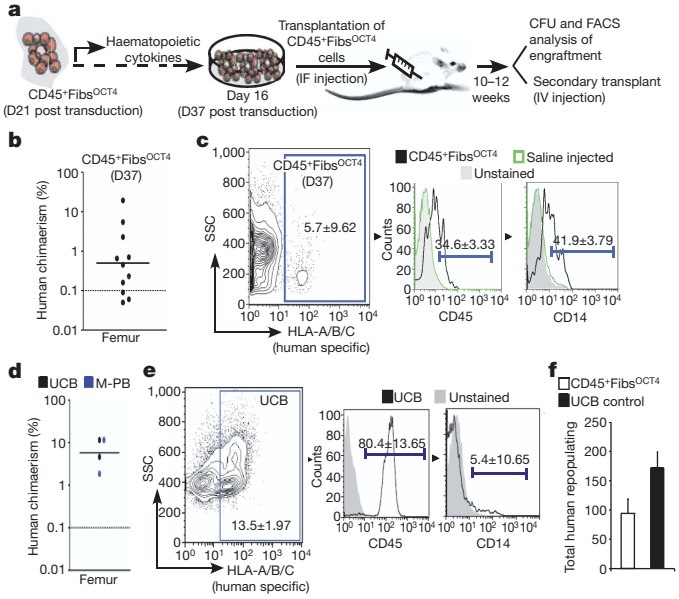

Figure 4 | *In vivo* capacity of CD45$^+$Fibs^{OCT4}. a, Schematic of NOD/SCID IL2Rγc-null mice xenograft model for injection of CD45$^+$FibsOCT4. **b**, Graph representing human chimaerism of CD45$^+$FibsOCT4 treated with cytokines ($n = 12$). **c**, FACS histograms of engrafted CD45$^+$FibsOCT4 showing the presence of CD45$^+$ and CD14$^+$ population ($n = 12$). **d**, Graph representing human chimaerism of UCB derived progenitors and MPB cells ($n = 4$). **e**, Representative FACS histograms of engrafted UCB and MPB cells, showing the presence of CD45$^+$ and CD14$^+$ population ($n = 4$). **f**, CFU capacity of engrafted CD45$^+$FibsOCT4 versus UCB ($n = 3$).

of limited engraftment ability in secondary recipient NSG mice (Supplementary Fig. 14b), indicating that they do not possess transformed leukaemic stem cell properties[21], and thus represent safer haematopoietic transplantation product alternatives, as compared to hPSC-derived cells that retain tumour potential[22,23]. Collectively, our data indicate that CD45$^+$FibsOCT4 can give rise to functional haematopoietic progenitor-like cells that are able to mature into myeloid lineages *in vitro* and *in vivo*.

Erythroid and megakaryocytic potential of CD45$^+$ Fibs

Despite the ability to derive all myeloid lineages from CD45$^+$FibsOCT4, erythroid cells were not detected. On OCT4 transduction, Fibs expressed the erythroblast marker CD71 at a frequency of nearly 40% (Fig. 5a). As Erythropoietin (EPO) induces early erythroid differentiation[24], we added EPO to FibOCT4 cultures, and observed a twofold increase in the number of Fibs expressing CD71, along with an increase in expression of Glycophorin-A (Fig. 5b) and adult β-globin protein (Fig. 5c). In contrast, Fibs (Fig. 5c) and hPSC-derived haematopoietic cells (Fig. 5c inset) lacked β-globin protein. In the absence of EPO, only β-globin transcript was expressed in the CD45$^+$FibsOCT4 (Fig. 5d), while β-globin protein was undetectable (Fig. 5c). In contrast, and unlike haematopoietic cells derived from hPSCs[25], haematopoietic cells derived from CD45$^+$FibsOCT4 lacked embryonic globin expression and expressed modest levels of fetal globin (Fig. 5d). EPO-treated CD45$^+$FibsOCT4 exhibited both primitive and mature erythrocyte (enucleated) morphologies (Fig. 5e) and allowed for erythroid progenitor emergence, detected by colony formation (BFU-E) and CFU-Mixed colonies (CFU-Mix; dual myeloid and erythroid capacity), similar to that for UCB, without reduction in monocytic or granulocytic progenitor capacity (Fig. 5f, g, Supplementary Fig. 15a, b).

Studies have indicated that erythroid and megakaryocytic lineage commitment occur together and potentially arise from a common precursor population[26,27]. EPO stimulation of CD45$^+$FibsOCT4 induced emergence of megakaryocytic lineage, as detected by Megakaryocytic (Mk)-CFU assay[28], indicated by the presence of Mk-specific antigen GPllb/llla (CD41; red/pink colonies) (Fig. 5h right panel, Fig. 5i), while

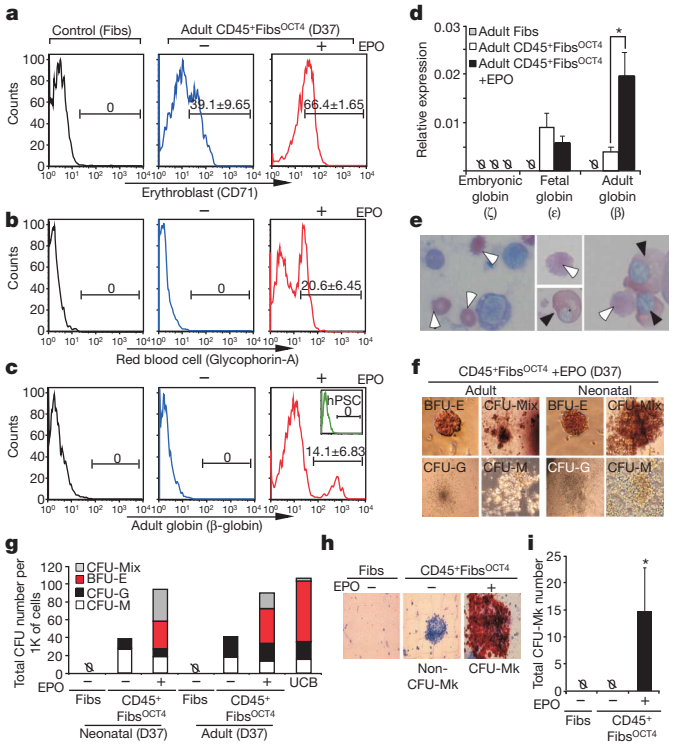

Figure 5 | EPO treated CD45$^+$Fibs^{OCT4} generate erythroid and megakaryocytic progenitors. **a–c,** Representative FACS histograms of erythroblast marker, CD71 (**a**), Glycophorin-A (**b**) and adult-globin (**c**; upper panel, differentiated hPSCs) in Fibs and CD45$^+$Fibs^{OCT4} with and without EPO ($n = 3$). **d**, Relative mRNA expression of embryonic, fetal and adult-globins ($n = 3$; $^*P < 0.001$). **e**, Giemsa-Wright stained EPO treated CD45$^+$Fibs^{OCT4} showing primitive (black arrow) and mature (white arrow) erythrocyte morphologies. **f**, CFU images, and **g**, quantitative analysis of CFU formation of EPO treated adult and neonatal CD45$^+$Fibs^{OCT4} (20×; $n = 3$). (Erythroid blast forming units, BFU-E; all lineages, CFU-Mix). **h**, Megakaryocytic CFU (CFU-Mk) images (CD41$^+$ cells; 20×), and **i**, quantification ($n = 3$; $^*P < 0.001$). 0, not detected.

this haematopoietic progenitor type was absent in CD45$^+$Fibs^{OCT4} without EPO (Fig. 5h middle panel, Fig. 5i) or control Fibs (Fig. 5h left panel, Fig. 5i). Taken together, EPO treatment induces definitive and not primitive (embryonic) haematopoietic programs[29], and reveals megakaryocytic lineage during conversion of Fibs to haematopoietic fate.

OCT4 haematopoietic program from Fibs

To develop a broader understanding of the role of OCT4 during haematopoietic conversion of Fibs (Fig. 6a), we examined gene expression and OCT4 occupancy over the time course of CD45$^+$ cell emergence and maturation. As early as day (D) 4 post transduction, significant changes occur in molecular pathways, including metabolic and developmental processes (Supplementary Fig. 16a). Furthermore, global gene expression of the Fibs over the course of CD45$^+$ cell emergence (D0, D4 and D21) indicated a decrease in fibroblast-specific gene expression[15] (Fig. 6b), without pluripotency gene induction (Fig. 6c), excluding OCT4. Fibs^{OCT4} immediately upregulated haematopoietic cytokine receptors, including FLT3 and KIT, receptors of FLT3LG and SCF, respectively (Fig. 6d), along with transcription factors associated with early haematopoietic development (Fig. 6e, Supplementary Fig. 16b, c). In addition, Fibs possess low to undetectable levels of genes associated with pluripotency, such as NANOG and SOX2, or haematopoietic specification, such as SCL/TAL1, RUNX1, C/EBPα, GATA1 or PU.1/SPI1 (refs 6, 30–32) (Fig. 6f, Supplementary Fig. 17a). However, transduction with OCT4 was accompanied by a substantial increase of SCL, C/EBPα, GATA1 and RUNX1 (Fig. 6f). Interestingly, PU.1 and MIXL1, which were previously shown to regulate primitive blood development[6,33,34], were not differentially regulated (Fig. 6e, f, Supplementary Fig. 16b, c). Expression of genes associated with mesodermal transition from the pluripotent state, such as Brachyury and GATA2, were absent in both Fibs and CD45$^+$Fibs^{OCT4} (Fig. 6f), indicating that haematopoietic specification from Fibs does not involve embryonic-mesodermal transitions[35,36]. Molecular analysis of cytokine treated CD45$^+$Fibs^{OCT4} (D37) revealed reduced OCT4 levels, while maintaining RUNX1, SCL and C/EBPα levels (Supplementary Fig. 17b), and expression of all adult globins, including haemoglobin-α, β and δ (Supplementary Fig. 17c, Fig. 5d).

Like OCT4, OCT1 and OCT2 are also able to regulate haematopoietic-specific genes (Supplementary Fig. 18)[37–41]. While expression of OCT4 increased during CD45$^+$ cell emergence, followed by a significant reduction on cytokine treatment, the levels of OCT2 and OCT1 remained unchanged (Fig. 6g), suggesting that OCT4 does not target other Oct family members. Nevertheless, OCT1, OCT2 and OCT4 have the potential to bind the same octamer (POU) binding sequences in a cell context specific manner, thereby raising the possibility that OCT4 has the capacity to bind and potentially regulate gene targets of OCT1 and OCT2 (refs 37–40) (Fig. 6h, Supplementary Fig. 18). Thus, we examined OCT4 occupancy of haematopoietic, non-haematopoietic and pluripotency genes that contain shared OCT1, OCT2 or OCT4 binding sequences in their putative promoters/enhancers (Fig. 6h, Supplementary Fig. 18). Consistent with changes in gene expression (Fig. 6f), RUNX1, SCL, CD45 and GATA1 displayed substantial OCT4 occupancy (Fig. 6i). To assess the specificity of OCT4 occupancy of haematopoietic targets during CD45$^+$ cell emergence, we examined non-haematopoietic associated promoters previously shown to bind OCT1 or OCT2. Consistent with global gene expression (Supplementary Fig. 7a), housekeeping genes GADD45A and POLR2A exhibited an increase in OCT4 occupancy at their respective promoters, while non-haematopoietic genes MYF5 and NKX2.5, associated with mesodermal development, did not (Fig. 6j). In contrast to hPSCs, OCT4 did not occupy NANOG, MYC and TBX3 promoters (Fig. 6k) in CD45$^+$Fibs^{OCT4}. While OCT4 binds its own promoter (Fig. 6k), it does not bind the OCT2 promoter (Fig. 6i), consistent with OCT2 expression (Supplementary Fig. 5a, b). Collectively, these temporal gene expression analyses along with OCT4 occupancy studies demonstrate that ectopic OCT4 expression orchestrates haematopoietic program potential in Fibs towards blood fate conversion.

Discussion

Our current study demonstrates the ability of human fibroblasts to be directly converted to multipotent haematopoietic progenitors of the myeloid, erythroid and megakaryocytic lineages via OCT4-dependent cellular programming without traversing the pluripotent state or activation of mesodermal pathways[35,36]. Given that transition from primitive to definitive haematopoiesis is delineated by the shift from embryonic to adult haemoglobin expression[29], our study demonstrates that unlike hPSC-derived haematopoietic cells[42], CD45$^+$Fibs exclusively acquire adult-globin protein indicative of definitive haematopoietic program activation. Acquisition of the haematopoietic phenotype is linked to the direct binding of OCT4 to the regulatory loci of haematopoietic-specific genes[37,40,41,43]. While OCT1 and OCT2 have been shown to play a role in adult lymphopoiesis[10–12], OCT4 has not been implicated in blood fate. Given the conservation between the native or predicted octamer binding sequences among OCT1, OCT2 and OCT4, it is highly possible that POU domains shared among OCT proteins have a redundant role in haematopoietic fate conversion. Although OCT4 converts fibroblasts to myeloid and erythroid progenitors, lymphoid fate was not detected. Accordingly, it is plausible that ectopic expression of OCT4, OCT1 and OCT2, coupled with lymphoid specific culture conditions, may support lymphoid conversion from Fibs, and is currently being pursued.

Although recent reports demonstrate conversion of mouse fibroblasts to neural, cardiac and macrophage-like cells[6–8], the present

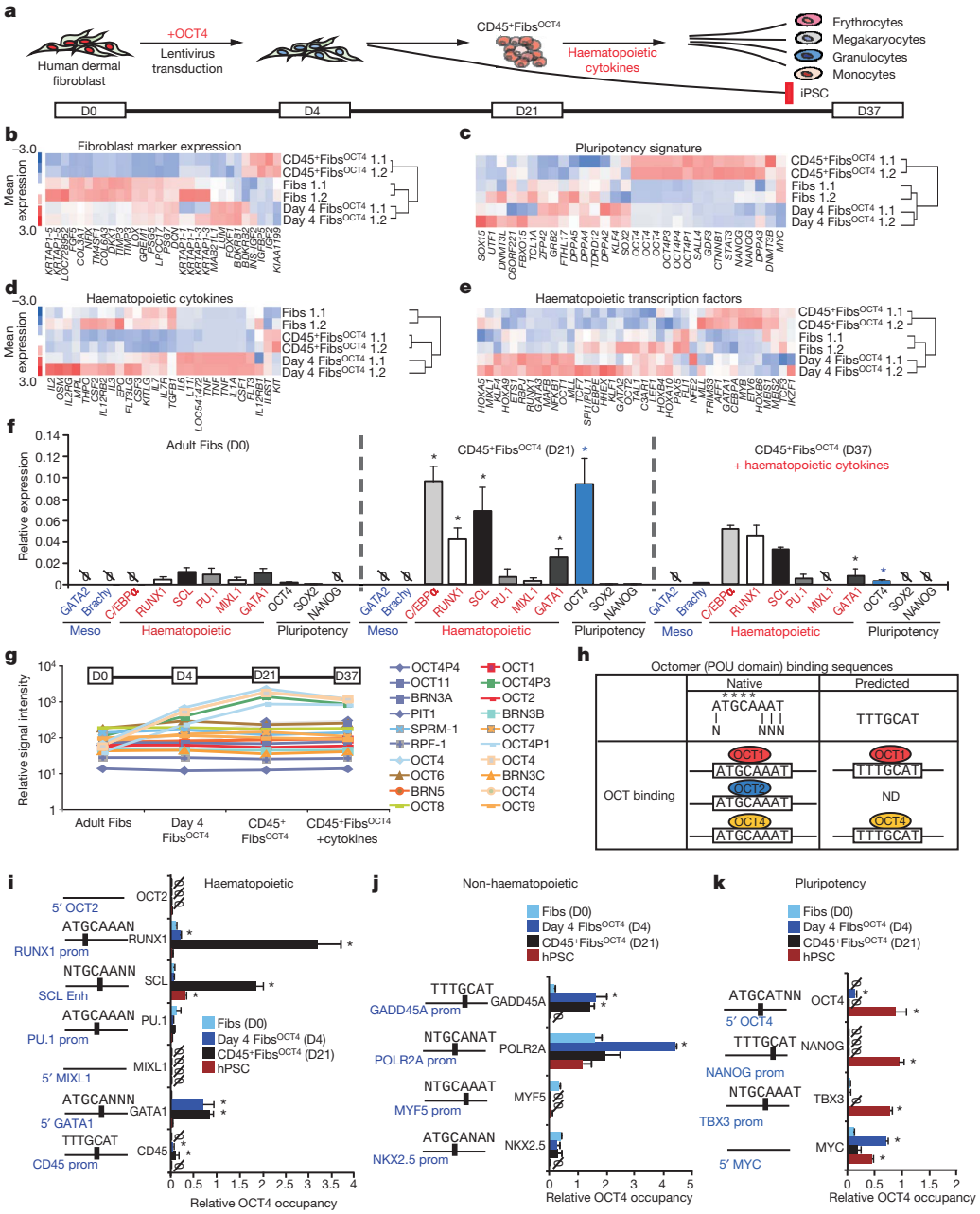

Figure 6 | OCT4 causes haematopoietic program activation in Fibs. a, Proposed model for haematopoietic fate conversion from $CD45^{+}Fibs^{OCT4}$ (D0 to D37). **b**–**e**, Global gene expression based on fibroblast marker expression (**b**), pluripotency signature (**c**), haematopoietic cytokines (**d**) and haematopoietic transcription factors (**e**). **f**, Relative mRNA expression of mesodermal, haematopoietic specific and pluripotency genes at D0 versus D21 and D37 ($n = 4$, $^{*}P < 0.001$). **g**, Gene expression profile of OCT (POU) genes. **h**, Schematic of native and predicated octamer binding sequences for OCT4, OCT1 and OCT2, (N, any nucleotide; starred/underlined, conserved octamer-binding region). **i**–**k**, Right panels: relative OCT4 occupancy of haematopoietic specific (**i**), non-haematopoietic (**j**) and pluripotency (**k**) gene enhancer/promoter regions ($n = 3$; $^{*}P < 0.001$). **i**–**k**, Left panels: proximity maps of primers (arrows) relative to native or predicted octamer-binding region (black box).

study uniquely demonstrates the ability to generate multipotent, rather than unipotent (single lineage), cell types from fibroblasts in the human, hence establishing future clinical utility of these multipotent cells of the haematopoietic lineage. Taking into account the yield, expansion capacity and clinical feasibility[44] of using this direct conversion approach to haematopoietic fate (Supplementary Table 2), our technique could provide a reasonable basis for autologous cell replacement therapies.

METHODS SUMMARY

Cultures. Adult and neonatal dermal fibroblasts were cultured in F12-DMEM media supplemented with (1) IGFII and bFGF, or (2) IGFII, bFGF, Flt3 and SCF, on Matrigel-coated plates. Lentiviral vectors (pSIN) containing cDNAs of OCT4, NANOG, SOX2 and LIN28 were obtained from Addgene and were transfected into 293-FT cells using the virapower packaging kit (Invitrogen). Fibroblast transductions were performed at 24 h post 10^{4} seeding on Matrigel. For derivation of $CD45^{+}$ cells, fibroblasts were transduced with OCT4 expressing lentivirus and cultured in media (1) or (2), and iPSCs were derived as previously described[15]. Further haematopoietic differentiation was carried out using EB media supplemented with haematopoietic cytokines.

Functional/phenotype analysis. Flow cytometry analysis of haematopoietic and pluripotency markers was performed using FACSCalibur (Beckman Coulter), and analysis was performed using the FlowJo 8.8.6 software. Cell sorting was performed using FACSAria II (Becton-Dickinson); Histological profiling of haematopoietic cells was performed using Cytospin and Giemsa-Wright staining and confirmed by the McMaster Pathology and Hematology Group; CFU formation was assayed using Methocult and Megacult kits from Stem Cell Technologies;

Macrophage phagocytosis assay was performed using Fluorescein conjugated-latex beads (Sigma) as particle tracers to analyse uptake by monocytes derived from $CD45^{+}Fibs^{OCT4}$ cells; *in vivo* engraftment capacity was evaluated by intrafemoral injection of $CD45^{+ve}$ cells into NSG mice. Ten weeks later bone marrow from injected femur, contralateral bones and spleen was analysed for the presence of human cells by flow cytometry; teratoma formation was evaluated by intratesticular injection into NOD/SCID mice. Resulting teratomas were evaluated for the presence of mesoderm, endoderm and ectoderm through histological examination.

Molecular analysis. For qPCR and microarray analysis, RNA was extracted using a total RNA purification kit (Norgen). Microarray analysis was done using Human Gene 1.0 ST arrays (Affymetrix) and dChIP software. OCT4 DNA occupancy (OCT4 ChIP) was done as previously described[45]. See Supplementary Methods for additional details.

Full Methods and any associated references are available in the online version of the paper at www.nature.com/nature.

Received 17 August; accepted 20 October 2010.
Published online 7 November 2010.

1. Jaenisch, R. & Young, R. Stem cells, the molecular circuitry of pluripotency and nuclear reprogramming. *Cell* **132,** 567–582 (2008).
2. Chan, E. M. *et al.* Live cell imaging distinguishes bona fide human iPS cells from partially reprogrammed cells. *Nature Biotechnol.* **27,** 1033–1037 (2009).
3. Lin, T. *et al.* A chemical platform for improved induction of human iPSCs. *Nature Methods* **6,** 805–808 (2009).
4. Mikkelsen, T. S. *et al.* Dissecting direct reprogramming through integrative genomic analysis. *Nature* **454,** 49–55 (2008).
5. Kanawaty, A. & Henderson, J. Genomic analysis of induced pluripotent stem (iPS) cells: routes to reprogramming. *Bioessays* **31,** 134–138 (2009).
6. Feng, R. *et al.* PU.1 and C/EBPα/β convert fibroblasts into macrophage-like cells. *Proc. Natl Acad. Sci. USA* **105,** 6057–6062 (2008).
7. Vierbuchen, T. *et al.* Direct conversion of fibroblasts to functional neurons by defined factors. *Nature* **463,** 1035–1041 (2010).
8. Ieda, M. *et al.* Direct reprogramming of fibroblasts into functional cardiomyocytes by defined factors. *Cell* **142,** 375–386 (2010).
9. Kang, J., Shakya, A. & Tantin, D. Stem cells, stress, metabolism and cancer: a drama in two Octs. *Trends Biochem. Sci.* **34,** 491–499 (2009).
10. Brunner, C. *et al.* B cell-specific transgenic expression of Bcl2 rescues early B lymphopoiesis but not B cell responses in BOB.1/OBF.1-deficient mice. *J. Exp. Med.* **197,** 1205–1211 (2003).
11. Emslie, D. *et al.* Oct2 enhances antibody-secreting cell differentiation through regulation of IL-5 receptor α chain expression on activated B cells. *J. Exp. Med.* **205,** 409–421 (2008).
12. Pfisterer, P. *et al.* CRISP-3, a protein with homology to plant defense proteins, is expressed in mouse B cells under the control of Oct2. *Mol. Cell. Biol.* **16,** 6160–6168 (1996).
13. Takahashi, K. *et al.* Induction of pluripotent stem cells from adult human fibroblasts by defined factors. *Cell* **131,** 861–872 (2007).
14. Takahashi, K. & Yamanaka, S. Induction of pluripotent stem cells from mouse embryonic and adult fibroblast cultures by defined factors. *Cell* **126,** 663–676 (2006).
15. Yu, J. *et al.* Induced pluripotent stem cell lines derived from human somatic cells. *Science* **318,** 1917–1920 (2007).
16. Hassan, H. T. & Zander, A. Stem cell factor as a survival and growth factor in human normal and malignant hematopoiesis. *Acta Haematol.* **95,** 257–262 (1996).
17. Lyman, S. D. *et al.* Molecular cloning of a ligand for the flt3/flk-2 tyrosine kinase receptor: a proliferative factor for primitive hematopoietic cells. *Cell* **75,** 1157–1167 (1993).
18. Kim, J. B. *et al.* Direct reprogramming of human neural stem cells by OCT4. *Nature* **461,** 649–653 (2009).
19. Lebofsky, R. & Walter, J. C. New Myc-anisms for DNA replication and tumorigenesis? *Cancer Cell* **12,** 102–103 (2007).
20. Silverstein, S. C., Steinman, R. M. & Cohn, Z. A. Endocytosis. *Annu. Rev. Biochem.* **46,** 669–722 (1977).
21. Hope, K. J., Jin, L. & Dick, J. E. Acute myeloid leukemia originates from a hierarchy of leukemic stem cell classes that differ in self-renewal capacity. *Nature Immunol.* **5,** 738–743 (2004).
22. Roy, N. S. *et al.* Functional engraftment of human ES cell-derived dopaminergic neurons enriched by coculture with telomerase-immortalized midbrain astrocytes. *Nature Med.* **12,** 1259–1268 (2006).
23. Amariglio, N. *et al.* Donor-derived brain tumor following neural stem cell transplantation in an ataxia telangiectasia patient. *PLoS Med.* **6,** e1000029 (2009).
24. Fried, W. Erythropoietin and erythropoiesis. *Exp. Hematol.* **37,** 1007–1015 (2009).
25. Perlingeiro, R. C., Kyba, M. & Daley, G. Q. Clonal analysis of differentiating embryonic stem cells reveals a hematopoietic progenitor with primitive erythroid and adult lymphoid-myeloid potential. *Development* **128,** 4597–4604 (2001).
26. Debili, N. *et al.* Characterization of a bipotent erythro-megakaryocytic progenitor in human bone marrow. *Blood* **88,** 1284–1296 (1996).
27. Klimchenko, O. *et al.* A common bipotent progenitor generates the erythroid and megakaryocyte lineages in embryonic stem cell-derived primitive hematopoiesis. *Blood* **114,** 1506–1517 (2009).
28. Strodtbeck, D. *et al.* Graft clonogenicity and intensity of pre-treatment: factors affecting outcome of autologous peripheral hematopoietic cell transplantation in patients with acute myeloid leukemia in first remission. *Bone Marrow Transplant.* **36,** 1083–1088 (2005).
29. Orkin, S. H. & Zon, L. I. Hematopoiesis and stem cells: plasticity versus developmental heterogeneity. *Nature Immunol.* **3,** 323–328 (2002).
30. Shivdasani, R. A., Mayer, E. L. & Orkin, S. H. Absence of blood formation in mice lacking the T-cell leukaemia oncoprotein tal-1/SCL. *Nature* **373,** 432–434 (1995).
31. Ichikawa, M., Asai, T., Chiba, S., Kurokawa, M. & Ogawa, S. Runx1/AML-1 ranks as a master regulator of adult hematopoiesis. *Cell Cycle* **3,** 722–724 (2004).
32. Friedman, A. D. Transcriptional control of granulocyte and monocyte development. *Oncogene* **26,** 6816–6828 (2007).
33. Koschmieder, S., Rosenbauer, F., Steidl, U., Owens, B. M. & Tenen, D. G. Role of transcription factors C/EBPα and PU.1 in normal hematopoiesis and leukemia. *Int. J. Hematol.* **81,** 368–377 (2005).
34. Ng, E. S. *et al.* The primitive streak gene Mixl1 is required for efficient haematopoiesis and BMP4-induced ventral mesoderm patterning in differentiating ES cells. *Development* **132,** 873–884 (2005).
35. Tsai, F. Y. *et al.* An early haematopoietic defect in mice lacking the transcription factor GATA-2. *Nature* **371,** 221–226 (1994).
36. Vijayaragavan, K. *et al.* Noncanonical Wnt signaling orchestrates early developmental events toward hematopoietic cell fate from human embryonic stem cells. *Cell Stem Cell* **4,** 248–262 (2009).
37. Boyer, L. A. *et al.* Core transcriptional regulatory circuitry in human embryonic stem cells. *Cell* **122,** 947–956 (2005).
38. Kistler, B., Pfisterer, P. & Wirth, T. Lymphoid- and myeloid-specific activity of the PU.1 promoter is determined by the combinatorial action of octamer and ets transcription factors. *Oncogene* **11,** 1095–1106 (1995).
39. Rodda, D. J. *et al.* Transcriptional regulation of nanog by OCT4 and SOX2. *J. Biol. Chem.* **280,** 24731–24737 (2005).
40. Sridharan, R. *et al.* Role of the murine reprogramming factors in the induction of pluripotency. *Cell* **136,** 364–377 (2009).
41. Ghozi, M. C., Bernstein, Y., Negreanu, V., Levanon, D. & Groner, Y. Expression of the human acute myeloid leukemia gene AML1 is regulated by two promoter regions. *Proc. Natl Acad. Sci. USA* **93,** 1935–1940 (1996).
42. Chang, K. H. *et al.* Definitive-like erythroid cells derived from human embryonic stem cells coexpress high levels of embryonic and fetal globins with little or no adult globin. *Blood* **108,** 1515–1523 (2006).
43. Kwon, U. K., Yen, P. H., Collins, T. & Wells, R. A. Differential lineage-specific regulation of murine CD45 transcription by Oct-1 and PU.1. *Biochem. Biophys. Res. Commun.* **344,** 146–154 (2006).
44. Feugier, P. *et al.* Hematologic recovery after autologous PBPC transplantation: importance of the number of postthaw CD34+ cells. *Transfusion* **43,** 878–884 (2003).
45. Rampalli, S. *et al.* p38 MAPK signaling regulates recruitment of Ash2L-containing methyltransferase complexes to specific genes during differentiation. *Nature Struct. Mol. Biol.* **14,** 1150–1156 (2007).

Supplementary Information is linked to the online version of the paper at www.nature.com/nature.

Acknowledgements This work was supported by grants to M.B. from the Canadian Institute of Health Research (CIHR), the Canadian Cancer Society Research Institute (CCS-RI), the StemCell Network and the Ontario Ministry of Research Innovation (MRI). M.B. is supported by the Canadian Chair Program and holds the Canada Research Chair in human stem cell biology. E.S. is supported by Ministry of Research and Innovation (MRI) and MITACS fellowships, R.M.R is supported by a CCS-RI fellowship and R.M. is supported by an Ontario Graduate Scholarship (OGS). We thank T. Werbowetski-Ogilvie for her help.

Author Contributions All authors contributed to the acquisition, analysis and interpretation of the data; E.S., S.R., R.M.R. and M.B. initiated and designed the study; A.S. performed Affymetrix analyses; R.M.R. performed *in vivo* analyses; E.S., S.R., R.M.R. and M.B. wrote the paper.

Author Information Data are available on the NCBI Gene Expression Omnibus (GEO) and are accessible through GEO Series accession number GSE24621. Reprints and permissions information is available at www.nature.com/reprints. The authors declare no competing financial interests. Readers are welcome to comment on the online version of this article at www.nature.com/nature. Correspondence and requests for materials should be addressed to M.B. (mbhatia@mcmaster.ca).

METHODS

Cell culture. Primary human dermal adult fibroblasts derived from breast dermal tissue, and neonatal fibroblasts derived from foreskin tissue, were initially maintained in fibroblast medium (DMEM (Gibco)) supplemented with 10% v/v FBS (Neonatal Bovine Serum, HyClone), 1 mM L-glutamine (Gibco), and 1% v/v non-essential amino acids (NEAA; Gibco) before transduction with OCT4 lentivirus vector. Human dermal fibroblasts transduced with OCT4 were maintained on matrigel-coated dishes in complete F12 medium (F12 DMEM; Gibco) supplemented with 10% knockout serum replacement (Gibco), 1% NEAA (Gibco), 1 mM L-glutamine (Gibco), and 0.1 mM β-mercaptoethanol containing 16 ng ml^{-1} bFGF (BD Biosciences) and 30 ng ml^{-1} IGFII (Millipore), or in complete F12 medium containing 16 ng ml^{-1} bFGF and 30 ng ml^{-1} IGFII and supplemented with 300 ng ml^{-1} Flt-3 (R&D Systems) and 300 ng ml^{-1} stem cell factor (SCF; R&D Systems), for 21 days. The arising CD45^{+} OCT-transduced cells were transferred onto low attachment 24-well plates in haematopoietic medium, consisting of 80% knockout DMEM (KO-DMEM) (Gibco), 20% v/v non-heat inactivated fetal calf serum (FCS) (HyClone), 1% v/v NEAA, 1 mM L-glutamine and 0.1 mM β-mercaptoethanol (Sigma), for 16 days. Cultures were replaced with haematopoietic differentiation medium with cytokines (SCF, G-CSF, FLT3LG, IL-3, IL-6 and BMP-4; R&D Systems), or for erythroid/megakaryocytic differentiation the medium was supplemented with haematopoietic cytokines plus 3 U ml^{-1} EPO and changed every 4 days. This was followed by collection for molecular and functional analysis.

Lentivirus production. Lentiviral vectors (pSIN) containing cDNAs of OCT4, NANOG, SOX2 and Lin-28 were obtained from Addgene. These vectors were transfected with virapower packaging kit from Invitrogen in a 293-FT packaging cells line. Viral supernatants were harvested 48 h after transfection and ultracentrifuged to concentrate the virus. An equal amount of each virus was used for fibroblast transduction in the presence of 8 μg ml^{-1} polybrene.

Lentivirus transduction. For generation of cells containing single transcription factors, human adult dermal fibroblasts (Fibs) (derived from breast skin; age 30–40 yr) or neonatal foreskin Fibs were seeded at a density of 10,000 cells per well on matrigel coated 12-well plates. Twenty-four hours after seeding, Fibs were infected with lentivirus expressing either OCT4 or NANOG or SOX2 (NANOG and SOX2 transduction was only performed for adult dermal Fibs). Transduced fibroblasts were then grown in complete F12 medium containing 16 ng ml^{-1} bFGF and 30 ng ml^{-1} IGFII supplemented with 300 ng ml^{-1} Flt-3 and 300 ng ml^{-1} SCF, or complete F12 medium containing 16 ng ml^{-1} bFGF and 30 ng ml^{-1} IGFII alone, for up to 21 days. Emerging CD45^{+} colonies were counted 14–21 days after infection. Colonies were picked manually and maintained on matrigel-coated wells. Molecular analysis was done on purified untransduced Fibs (D0), OCT4 transduced Fibs at day 4 (D4), CD45^{+} Fibs at day 21 (D21) and haematopoietic cytokine treated or untreated CD45^{+} Fibs at day 37 (D37). Day 4 post OCT4 transduction was chosen as the early event time point, based on a number of criteria: optimal time for recovery following transduction; visible morphological changes within the culture; and resumption of normal cell cycle kinetics. The day 4 OCT4 transduced Fibs (D4) were isolated by puromycin selection overnight (OCT4 vector contains a puromycin resistance cassette), and the purity of the sample was validated by staining for OCT4 followed by OCT4 expression analysis using flow cytometry; samples used for molecular analysis exhibited 99% OCT4 levels. The D21 and D37 CD45^{+}Fibs^{OCT4} were isolated on the basis of their CD45 expression. D21 and D37 cells were stained with CD45-APC antibody (BD Biosciences) and sorted using a FACSAria II (Becton Dickinson); samples used for molecular analysis exhibited 99% CD45 levels.

Induction of reprogramming. For generation of reprogrammed cells from fibroblasts, cells were seeded at the density of 10,000 cells per well on matrigel coated 12-well plates. Twenty-four hours after seeding, fibroblasts were transduced with lentivirus expressing OCT4/NANOG/SOX2/LIN28 (ref. 15). Transduced fibroblasts were then grown in F12 medium supplemented with 30 ng ml^{-1} IGFII and 16 ng ml^{-1} bFGF. Reprogrammed iPSC colonies were counted four weeks post infections. Colonies were picked manually and maintained on matrigel-coated wells.

Live staining. For live staining, sterile Tra-1-60 antibody (Millipore) was pre-conjugated with sterile Alexa Fluor-647 at room temperature. Reprogrammed colonies were washed once with F12 medium and incubated with Tra-1-60-Alexa 647 antibodies for 30 min at room temperature. Cultures were then washed twice to remove unbound antibody. Cells were visualized by an Olympus IX81 fluorescence microscope.

Flow cytometry. For pluripotency marker expression, cells were treated with collagenase IV, and then placed in cell dissociation buffer for 10 min at 37 °C (Gibco). Cell suspensions were stained with SSEA3 antibody (1:100) (Developmental Studies Hybridoma Bank, mAB clone MC-631, Univ. Iowa) or Tra-1-60-PE (1:100) antibody (BD Biosciences). For SSEA3 staining, Alexa Fluor-647 goat anti-rat IgM (1:1,000) (Molecular Probes, Invitrogen) was used as the secondary antibody. Live cells were identified by 7-amino actinomycin (7AAD) exclusion and then analysed for cell surface marker expression using a FACSCalibur (Becton Dickinson). Collected events were analysed using FlowJo 8.8.6 Software (Tree Star).

Cells from the haematopoietic differentiation medium were disassociated with TrypLE (Gibco) at D16 and analysed for expression of haematopoietic progenitor and mature haematopoietic markers. Haematopoietic cells were identified by staining single cells with fluorochrome-conjugated monoclonal antibodies (mAb): CD34-FITC and APC- or FITC-labelled anti-human CD45 (BD Biosciences), FITC-anti-CD33 (BD Pharmingen), PE-anti-CD13 (BD Pharmingen), PE- or FITC-anti-CD71 (BD Pharmingen), FITC-anti-HLA-A/B/C (BD Pharmingen), PE-anti-CD15 (BD Pharmingen), PE-anti-CD15 (BD Pharmingen); PE anti-CD14 (BD Pharmingen), FITC- or PE-anti-GlyA (BD Pharmingen), and APC- or PE-anti-β-globin (SantaCruz Biotech). The mAb and their corresponding isotypes were used at 1–2 mg ml^{-1}; optimal working dilutions were determined for individual antibodies. Frequencies of cells possessing the haemogenic and haematopoietic phenotypes were determined on live cells by 7AAD (Immunotech) exclusion, using FACSCalibur (Beckman Coulter), and analysis was performed using FlowJo 8.8.6 Software.

RT–PCR and qPCR. Total RNA was isolated using the Norgen RNA isolation kit. RNA was then subjected to cDNA synthesis using superscript III (Invitrogen). Quantitative PCR (qPCR) was performed using Platinum SYBR Green–UDP mix (Invitrogen). For the analysis of the sample, the threshold was set to the detection of Gus-B (β-glucuronidase)[46] and then normalized to internal control GAPDH. The base line for the experiment was set to the gene expression levels observed in fibroblasts. Given the expression of some of the genes within this starting population of fibroblasts, we felt that we should include the gene expression pattern for these cells. Hence, the data are represented as delta cycle threshold ($\Delta C(t)$) versus delta $\Delta C(t)$ ($\Delta\Delta C(t)$). (qPCR primer sequences are provided in Supplementary Table 3.)

Genomic DNA was isolated using the All In One isolation kit (Norgen). For integration studies, 150 ng genomic DNA was used per PCR reaction. PCR reactions were performed using 2X PCR Master Mix (Fermentas).

Affymetrix analysis. Total RNA was extracted from human dermal fibroblasts (2 replicates), puromycin selected day 4 OCT4 transduced fibroblasts (2 replicates) and sorted CD45^{+} cells (2 replicates) using the Total RNA Purification Kit (Norgen). RNA integrity was assessed using Bioanalyser (Agilent Technologies). Sample labelling and hybridization to Human Gene 1.0 ST arrays (Affymetrix) were performed by the Ottawa Health Research Institute Microarray Core Facility (OHRI). Affymetrix data were extracted, normalized, and summarized with the robust multi-average (RMA) method implemented in the Affymetrix Expression Console. CEL files were imported into dChIP software[47] for data normalization, extraction of signal intensities and probe-level analysis. All the data from each individual sample are available on the NCBI Gene Expression Omnibus (GEO, http://www.ncbi.nlm.nih.gov/geo/) and are accessible through GEO Series accession number GSE24621.

Chromatin immunoprecipitation. ChIP was performed as described previously[45]. Briefly, human pluripotent cells (H9 and iPSC1.2), human dermal fibroblast cells, puromycin selected day 4 OCT4 transduced cells, and sorted day 21 CD45^{+} cells were cross-linked using 1% formaldehyde. Chromatin was digested in buffer containing 0.1% SDS to obtain fragments of approximately of 1,000 bp length. Sonicated DNA was subjected to immunoprecipitation using anti-OCT4 (ChIP quality antibody; Cell Signaling Technology) and anti rabbit IgG antibodies (Santacruz Biotechnology). Immunoprecipitated DNA was further reverse cross-linked, purified and subjected to qPCR analysis using UDG-Platinum SYBR Green mix (Invitrogen). The promoter specific ChIP primers are listed in Supplementary Table 4. To calculate the relative enrichment, signals observed in control antibody were subtracted from signals detected from the specific antibody; the resulting differences were divided by signals observed from one-fiftieth of the ChIP input material.

Megakaryocyte assay. To detect human megakaryocytes, the MegaCult-C Complete Kit with Cytokines (Stem Cell Technologies) was used. The derivation of megakaryocytes was done according to instructions included with the kit. The kit includes pre-screened components for optimal growth of megakaryocyte CFUs, such as thrombopoietin (TPO), Interleukin-3 (IL-3), IL-6, IL-11 and SCF, chamber slides for growth and antibodies for subsequent immunocytochemical staining. In short, 10,000 CD45^{+} EPO treated cells were plated in the MegaCult medium containing the cocktail of growth factors mentioned above. The human CFU-Mks were detectable by day 10 to 15 and were subsequently fixed and stained according to protocol. Mk-specific antigen GPIIb/IIIa (CD41) linked to a secondary biotinylated antibody-alkaline phosphatase avidin conjugated detection system was used, where Mk-CFUs were red/pink in colour.

Cytospin. 1,000 $CD45^+$ OCT4 transduced cells were washed twice in cold 2% FBS in PBS and diluted in 500 µl of cold 1% FBS in PBS. The samples were loaded into the appropriate wells of the Cytospin centrifuge equipment. The samples were spun at 500 r.p.m. for 5 min to allow adherence to the slides. The slides were fixed with methanol for 1 min and allowed to dry for 30 min. Then slides were stained with Giemsa-Wright stain for 3 min, followed by 10 min in PBS and a quick wash in distilled water. The slides were allowed to dry overnight and mounted with mounting medium (Dako). Slides were viewed by an Olympus IX81 microscope. Blood cell typing/morphological criteria were confirmed by McMaster Pathology and Hematology.

Macrophage phagocytosis assay. Fluorescein (FITC) conjugated latex beads (Sigma) were used as particle tracers to analyse phagocytosis by monocytes derived from $CD45^+Fibs^{OCT4}$ cells treated with IL-4 and M-CSF. To measure phagocytosis, 10 µl of packed beads suspended in 3% FBS in PBS was added to 10^6 cells in Teflon tubes. After incubation for 90 min at 37 °C, cells were washed three times with cold PBS containing 3% FBS and 0.1% EDTA to remove free beads. The cells were then labelled to detect expression of CD45 (APC-conjugated) CD45 mAb together with FITC-bead uptake, and analysed by flow cytometry using FACSCalibur (BD) or visualized on tissue culture quality slides (VWR) and viewed by an Olympus IX81 fluorescence microscope.

Xenotransplant assays. NOD/SCID IL2Rγc null adult mice (NSG) were sub-lethally irradiated with 325 rads 24 h before transplantation. 5.0×10^5 $CD45^+$ OCT-transduced (D37) or human dermal fibroblasts or human mobilized peripheral blood or human umbilical cord blood lineage depleted cells were transplanted by intrafemoral injection. After 10 weeks, animals were culled, and bone marrow (BM) from injected femur, contralateral bones and spleen was analysed for the presence of human cells by flow cytometry (FACSCalibur, Becton Dickinson), followed by data analysis using FlowJo 8.8.6 Software (Tree Star). Cells positive for HLA-A/B/C and CD45 were analysed for the expression of haematopoietic lineage specific markers, such as CD14. For secondary transplants, total engrafted bone marrow cells were transplanted intravenously (IV injection) in adult irradiated NSG mice, as described for primary transplants. Genomic DNA from engrafted cells was then analysed using conventional PCR by primers specific for the α-satellite of human chromosome 17: forward, 5′-GGGATAATTTCAGCTGACTAAACAG-3′; reverse, 5′-TTCCGTTTAGTTAGGTGCAGTTATC-3′.

Methylcellulose colony-forming assay. Cells were plated at 1,000 FACSAria II sorted (Becton Dickinson) $CD45^+CD34^+$ cells or 5,000 total cells for EPO treatments were seeded in 1 ml of Methocult GF H4434 (Stem Cell Technologies). Colonies were scored after 14 days of culture using standard morphological criteria and analysed using the FACSCalibur (Becton Dickinson) for haematopoietic surface markers. Collected events were analysed using FlowJo 8.8.6 Software (Tree Star). For colony derivation from xenotransplant derived engrafted cells, the cells were first sorted based on HLA-A/B/C (BD Biosciences) followed by CD45 expression using a human specific anti-CD45 (BD Biosciences). The HLA-A/B/C and CD45 double positive cells were then plated at a density of 1,000 cell ml^{-1} in Methocult GF H4434. The colonies derived from engrafted cells were further analysed for haematopoietic surface markers using FACSAria II (Becton Dickinson). Collected events were analysed using FlowJo 8.8.6 Software (Tree Star).

Teratoma assay. The McMaster University Animal Care Council approved all procedures and protocols. Adult dermal fibroblasts, neonatal dermal (foreskin) fibroblasts, $CD45^+$ OCT4 transduced adult dermal fibroblasts, $CD45^+$ OCT4 transduced neonatal fibroblasts and iPSC 1.1 to 1.4 were treated with collagenase IV for 5–10 min, followed by collection and washing twice with saline and resuspended in saline. 500,000 cells per sample were injected intratesticularly into male NOD-SCID mice. Mice were killed 10–12 weeks after initial injection. Teratomas were extracted, embedded in paraffin and sectioned in 5-µm intervals followed by deparafinization in xylene and processing through a graded series of alcohol concentrations. Samples were stained with haematoxylin and eosin or OCT4 followed by dehydration and xylene treatment. Slides were mounted using Permount and imaged by scanning slides using Aperio Scan Scope; images were captured using Image Scope v9.0.19.1516 software. Tissue was also collected from a variety of organs including lung, spleen, liver, brain and kidney to investigate the presence of metastatic cells. Tissue typing was performed based on stringent histological and morphological criteria specific for each germ layer subtype. Mesoderm lineages, such as bone, were identified using presence of osteocytes and bone spicules (dark pink); cartilage was identified by the presence of chondrocytes and specific staining (light blue) of the extra cellular matrix. Endoderm lineages, such as intestinal lumens, were identified by the presence of goblet cells in the lumen epithelium. Ectoderm lineages, such as skin, were identified based on distinguishing cell layer morphologies (that is, stratified); brain or neural tube was identified based on specific histological criteria. The presence of the germ layers and tissue typing was confirmed by McMaster Pathology.

Statistical analysis. All tests were performed using InStat Version 3.0a statistical software (GraphPad Software). Descriptive statistics including mean and s.e.m. along with one-way ANOVAs, and two-tailed *t*-tests were used to determine significant differences. $P < 0.01$ was considered significant.

46. Oshima, A. *et al.* Cloning, sequencing, and expression of cDNA for human β-glucuronidase. *Proc. Natl Acad. Sci. USA* **84,** 685–689 (1987).
47. Li, C. & Wong, W. H. Model-based analysis of oligonucleotide arrays: expression index computation and outlier detection. *Proc. Natl Acad. Sci. USA* **98,** 31–36 (2001).